OPEN ACCESS Freely available online

PLOS ONE

The C-Terminus of Human Nucleotide Receptor P2X7 Is Critical for Receptor Oligomerization and N-Linked Glycosylation

Lisa E. Wickert[1], Joshua B. Blanchette[1], Noelle V. Waldschmidt[3], Paul J. Bertics[1], John M. Denu[1], Loren C. Denlinger[2], Lisa Y. Lenertz[3]*

1 Department of Biomolecular Chemistry, The University of Wisconsin-Madison, Madison, Wisconsin, United States of America, **2** Department of Medicine, The University of Wisconsin-Madison, Madison, Wisconsin, United States of America, **3** Department of Biology, St. Olaf College, Northfield, Minnesota, United States of America

Abstract

Background: The $P2X_7$ receptor binds extracellular ATP to mediate numerous inflammatory responses and is considered a potential biomarker and therapeutic target for diverse inflammatory and neurological diseases. $P2X_7$ contains many single nucleotide polymorphisms, including several mutations located within its intracellular C-terminal trafficking domain. Mutations within the trafficking domain result in attenuated receptor activity and cell surface presentation, but the mechanisms by which amino acid changes within this region promote altered $P2X_7$ function have not been elucidated.

Methods and Results: We analyzed the amino acid sequence of $P2X_7$ for any potential trafficking signals and found that $P2X_7$ contains putative Arg-X-Arg ER retention sequences. Alanine substitutions near or within these sequences were constructed, and we determined that single mutation of R574 and R578 but not R576 or K579 attenuates $P2X_7$-stimulated activation of ERK1/2 and induction of the transcription factors FosB and ΔFosB. We found that mutation of R578 within the trafficking domain to the naturally occurring Gln substitution disrupts $P2X_7$ localization at the plasma membrane and results in R578Q displaying a higher apparent molecular weight in comparison to wild-type receptor. We used the glycosidase endoglycosidase H to determine that this difference in mass is due in part to the R578Q mutant possessing a larger mass of oligosaccharides, indicative of improper N-linked glycosylation addition and/or trimming. Chemical cross-linking experiments were also performed and suggest that the R578Q variant also does not form trimers as well as wild-type receptor, a function required for its full activity.

Conclusions: These data demonstrate the distal C-terminus of $P2X_7$ is important for oligomerization and post-translational modification of the receptor, providing a mechanism by which mutations in the trafficking domain disrupt $P2X_7$ activity and localization at the plasma membrane.

Citation: Wickert LE, Blanchette JB, Waldschmidt NV, Bertics PJ, Denu JM, et al. (2013) The C-Terminus of Human Nucleotide Receptor P2X7 Is Critical for Receptor Oligomerization and N-Linked Glycosylation. PLoS ONE 8(5): e63789. doi:10.1371/journal.pone.0063789

Editor: William R. Abrams, New York University, United States of America

Received March 25, 2012; **Accepted** April 11, 2013; **Published** May 14, 2013

Funding: This work was supported by NIH grant 5 P01 HL088594 and postdoctoral fellowships from The Hartwell Foundation and the American Heart Association. The funders had no role in study design, data collection and analysis, decision to publish, or preparation of the manuscript.

Competing Interests: The authors have declared that no competing interests exist.

* E-mail: lenertz@stolaf.edu

Introduction

The ATP receptor $P2X_7$ is an important regulator of the inflammatory response and is considered a potential therapeutic target and biomarker for several inflammatory and neurological diseases [1–3]. $P2X_7$ is a member of the P2X family of ionotropic nucleotide receptors ($P2X_{1-7}$) and is expressed in several immune cells including monocytes, macrophages, and microglia [2,4]. Numerous $P2X_7$ knockout and pharmacological studies have demonstrated that $P2X_7$ is important in glomerulonephritis, rheumatoid arthritis, cigarette smoke-induced lung inflammation, and depression. In addition, several groups are attempting to correlate $P2X_7$ single nucleotide polymorphisms (SNPs) and/or $P2X_7$ activity levels with viral-induced loss of asthma control, susceptibility to tuberculosis, and bipolar disorder [2]. Thus, $P2X_7$ is gaining considerable interest as a pharmacological target for an array of diseases that have an inflammatory component.

$P2X_7$ is activated by millimolar concentrations of ATP, which can be found in microenvironments with tissue damage or infected cells. ATP binding to this ion channel stimulates the influx and efflux of cations, activation of mitogen activated protein kinases (MAPKs), the processing of inflammatory mediators, gene transcription, and sometimes apoptosis [5,6]. Specifically, activated $P2X_7$ can stimulate the influx of Ca^{2+} and Na^+ and the efflux of K^+, the processing of interleukin-1β (IL-1β) into its mature form, and the generation of reactive oxygen species (ROS). $P2X_7$ stimulation also results in activation of the MAPKs extracellular signal-regulated kinases 1/2 (ERK1/2) and the formation of a non-specific pore that allows the entry of molecules up to 900 Da [2,6]. In addition, $P2X_7$ agonists can activate and/or induce numerous transcription factors including cyclic-AMP response

element-binding protein (CREB), nuclear factor-κB (NF-κB), and the activating protein-1 (AP-1) members JunB, FosB and ΔFosB. $P2X_7$ ligands can also stimulate the expression of several immune mediators including IL-6, IL-8, vascular endothelial growth factor (VEGF), and cyclooxygenase-2 (COX-2) [2].

Although many studies have been performed to examine the contribution of $P2X_7$ to normal physiology, relatively less research has been conducted to understand the basic mechanisms of $P2X_7$ activity and how its domains regulate receptor function. $P2X_7$ possesses a trafficking domain within its C-terminus, encompassing amino acids 551–590 [7,8]. The trafficking domain contains several identified SNPs including R574H, R574C, R578G, R578Q, K579E, P582S, P582L, K583N and K583T (NCBI). We and others have demonstrated that mutations within the intracellular distal C-terminus of $P2X_7$ result in altered trafficking, attenuated pore formation, and reduced cation channel activity [6,7,9–11]. Specifically, it has been reported that single mutations at I568, C572, R574, R578, F581, and double mutation of R578 and K579 promote decreased $P2X_7$ cation channel and/or pore activity [7,9,10]. The aforementioned investigations have revealed that the wild-type residues are required for normal expression of $P2X_7$ at the cell membrane, but the mechanisms by which these mutations result in attenuated activity have not been elucidated.

In this report we present evidence that mutation of the polymorphic residue R578 to Gln, a SNP identified in the SNP500Cancer project (NCBI), disrupts $P2X_7$ oligomerization and results in improper addition and/or trimming of its N-linked glycosylation modifications, indicative of a potential processing defect in the endoplasmic reticulum (ER). According to the SNP500Cancer study, the R578Q polymorphism exhibits a heterozygosity frequency of 0.065 in Caucasians, but a larger data set is required to more accurately determine the frequency. In this study, we provide one of the first mechanisms to explain why the distal C-terminus of $P2X_7$ is important for its plasma membrane localization and activity.

Methods

Reagents

The $P2X_7$ agonist 2'(3')-*O*-(4-benzoylbenzoyl)-ATP (BzATP), tunicamycin, ionomycin, and phorbol 12-myristate 13-acetate (PMA) were obtained from Sigma (St. Louis, MO). Bis(sulfosuccinimidyl) suberate (BS^3) and disuccinimidyl suberate (DSS) were obtained from Thermo Fisher Scientific (Waltham, MA), and endoglycosidase H (Endo H) was purchased from New England Biolabs (Ipswich, MA). Unless noted otherwise, the anti-$P2X_7$ antibody was obtained from Santa Cruz Biotechnology (Santa Cruz, CA; cat. no. sc-25698), the anti-ERK1/2 antibody was purchased from Millipore (Billerica, MA; cat. no. 06–182), and the anti-vinculin antibody was from Sigma (cat. no. V4505). The anti-pERK1/2 antibody was purchased from Invitrogen (Carlsbad, CA; cat. no. 44680G), and the anti-FosB antibody was purchased from Cell Signaling Technology (Danvers, MA; cat. no. 2251). The anti-GRB2 antibody was purchased from Santa Cruz Biotechnology (cat.no. sc-255). The monoclonal anti-$P2X_7$ antibody used in flow cytometry was from Dr. Iain Chessell (Glaxo Smith-Kline, Herts, U.K.) [10], and the anti-$P2X_7$ antibody used in the EndoH assay was obtained from BD Biosciences (Franklin Lakes, NJ; discontinued). Alexa Fluor 488-labeled goat anti-mouse IgG was purchased from Life Technologies (Grand Island, NY; cat. no. A-11029), and PE-labeled mouse IgG2b isotype control was purchased from BD Biosciences (cat. no. 555058).

Cell Culture and Harvesting

HEK293 (American Type Culture Collection, Manassas, VA) were cultured in Dulbecco's modified Eagle's medium (DMEM) supplemented with 10% cosmic calf serum (CCS) (Mediatech, Herndon, VA), 1% L-glutamine, and 100 U/ml penicillin/streptomycin. Human monocytes were purified and cultured as described before [12]. The cells were incubated at 37°C under 5% CO_2. Cell lysates were generally prepared by harvesting the cells in 2X sample buffer (20 mM Tris-HCl pH 6.8, 2 mM EDTA, 2 mM DTT, 1 mM Na_3VO_4, 2% SDS, 20% glycerol, 0.2% bromophenol blue) followed by boiling and sonicating the samples.

$P2X_7$ Constructs

Full-length human $P2X_7$ (accession number AAH11913) was subcloned into pcDNA3. The $P2X_7$ point mutants were generated by site-directed mutagenesis using the following primers and their reverse complements. For the double mutation, the N-terminal amino acid was mutated first followed by mutation of the second residue.

P2X7 R469A 5′-GAAAGGAGGCGACTCCTGCATCCAGGGATAGC - 3′.

P2X7 R469A/R471A 5′- CTTAGAAAGGAGGCGACTCCTGCATCCGCGGATAGCC - 3′.

P2X7 R544A 5′- GATTCCACCAACAGCGCGCTGCGGCACTGTG - 3′.

P2X7 R574A 5′- CCAGCTGCTGCGCCTGGAGGATCC - 3′.

P2X7 R576A 5′- CTGCTGCCGCTGGGCGATCCGGAAAG - 3′.

P2X7 R578A 5′- CTGCCGCTGGAGGATCGCGAAAGAGTTTC - 3′.

P2X7 R578Q 5′- CTGGAGGATCCAGAAAGAGTTTCCGAA - 3′.

P2X7 K579A 5′- GGAGGATCCGGGCAGAGTTTCC - 3′.

Generation of Stable Cell Lines

HEK293 cells were transfected with pcDNA3 containing wild-type or mutant $P2X_7$ using FuGENE^{TM} 6 transfection reagent according to the manufacturer's instructions (Roche). The cells were then selected with 500 μg/mL G418 sulfate (Sigma) to obtain a resistant population.

YO-PRO-1 Dye Uptake Assay

HEK293 cells transiently or stably expressing the indicated constructs were cultured on glass cover slips coated with 0.01% poly-*l*-lysine (Sigma). The transient-expressing cells were transfected using FuGENE^{TM} 6 transfection reagent according to the manufacturer's instructions. The cells were stimulated at room temperature in potassium-glutamate buffer (130 mM K-glutamate, 20 mM HEPES-KOH (pH 7.4), 5 mM KCl, 0.1% BSA, 10 mM glucose) with 250 μM BzATP or HEPES buffer control for 10 min in the presence of 1 μM YO-PRO-1 (Molecular Probes, Eugene, OR). Potassium-glutamate buffer is known to facilitate robust YO-PRO-1 uptake in response to BzATP, as previously reported [13,14]. The cells were then treated with 10 mM $MgCl_2$ to close the pore, fixed with 4% paraformaldehyde and imaged with a Zeiss Axioplan 2 microscope at 63X magnification.

ERK1/2 Activation and FosB/ΔFosB Induction Assays

HEK293 cells were cultured in collagen I-coated wells. Cells for the ERK1/2 activation tests were stimulated with 250 μM BzATP or buffer control for 5 min and lysates were prepared as performed previously [15]. Similar to our previous study, cells for the FosB/

ΔFosB induction assays were treated with 250 μM BzATP or buffer control for 5 min, the medium was replaced, and the cells were harvested 2 h later [12]. Proteins from cell lysates were separated by electrophoresis on 10% sodium dodecyl sulfate (SDS)-polyacrylamide gels, transferred to polyvinylidene fluoride (PVDF) membranes and blocked in 5% nonfat dry milk. The membranes were probed with the indicated primary antibodies, incubated with secondary antibodies conjugated to horseradish peroxidase (Santa Cruz Biotechnology), and visualized by enhanced chemiluminescence. The fold changes in ERK1/2 activation and FosB/ΔFosB induction were determined using Adobe Photoshop CS4 Version 11.0 to compare the relative band intensities of the BzATP-stimulated samples with the buffer control-stimulated samples. The background intensity was subtracted from the value of the pERK1/2 and FosB/ΔFosB bands, and these adjusted values were normalized to a loading control prior to calculating the fold changes. For quantifying the relative levels of pERK1/2, the band intensities of both pERK1 and pERK2 were used in the calculations. For the FosB/ΔFosB calculations, the band intensities of full-length FosB and the observed ΔFosB species were included. ΔFosB reportedly exists as a phosphorylated protein [16].

Proteinase K Digestion Assay

HEK293 stable cell lines were cultured in 10 cm plates to subconfluency. The cells were then lifted from the plates by rinsing them with serum-free medium and pelleted at 200×*g*. The cells were gently suspended in serum-free DMEM and incubated with 200 μg/mL proteinase K at 37°C for 90 min. The samples were boiled for 10 min to inactivate proteinase K, 2X sample buffer was added, and the lysates were sonicated. The generation of the ~240 amino acid $P2X_7$ intracellular C-terminus was assessed by immunoblotting the lysates with an anti-$P2X_7$ antibody that was raised against the C-terminus of $P2X_7$.

Chemical Cross-linking

$P2X_7$ monomers were cross-linked using protocols modified from Boumechache *et al.* [17]. To cross-link protein from cell lysates, HEK293 stable cell lines were cultured to subconfluency and harvested in phosphate buffer saline (PBS) containing 1% Triton X-100. The cells were incubated on ice for 30 min, sonicated and centrifuged at 21,000 x *g* to remove the Triton-insoluble material. The samples were incubated with 500 μM BS^3 at room temperature for 30 min, and the reaction was quenched by the addition of 20 mM Tris HCl pH 7.5. An equal volume of 2X sample buffer was added, and ~50 μg of protein from the lysates were boiled for 2 min. The proteins were separated on 7.5% polyacrylamide gels containing SDS, transferred to PVDF membrane, and immunoblotted with anti-$P2X_7$ antibody to detect $P2X_7$ trimers.

To cross-link proteins expressed at the plasma membrane, HEK293 stable cell lines were cultured to subconfluency and treated with 500 μM BS^3 at room temperature or 37°C for 30 min. The cells were harvested in 2X sample buffer, sonicated, boiled, and immunoblotted as described above.

To cross-link intracellular proteins, HEK293 stable cell lines were treated with 500 μM DSS at 37°C for 30 min. The reaction was quenched by the addition of 20 mM Tris HCl pH 7.5, and the proteins were processed as described above.

The differences in the amount of wild-type $P2X_7$ and $P2X_7$ R578Q that formed trimers upon cross-linking were calculated and compared. Adobe Photoshop CS4 Version 11.0 was used to obtain the relative band intensities of the $P2X_7$ monomers, $P2X_7$ trimers, and vinculin (loading control). The $P2X_7$ trimer values were normalized to the relative expression levels of the monomers. The adjusted values for the $P2X_7$ trimers were then normalized to vinculin, and Student's *t*-tests were performed to determine the

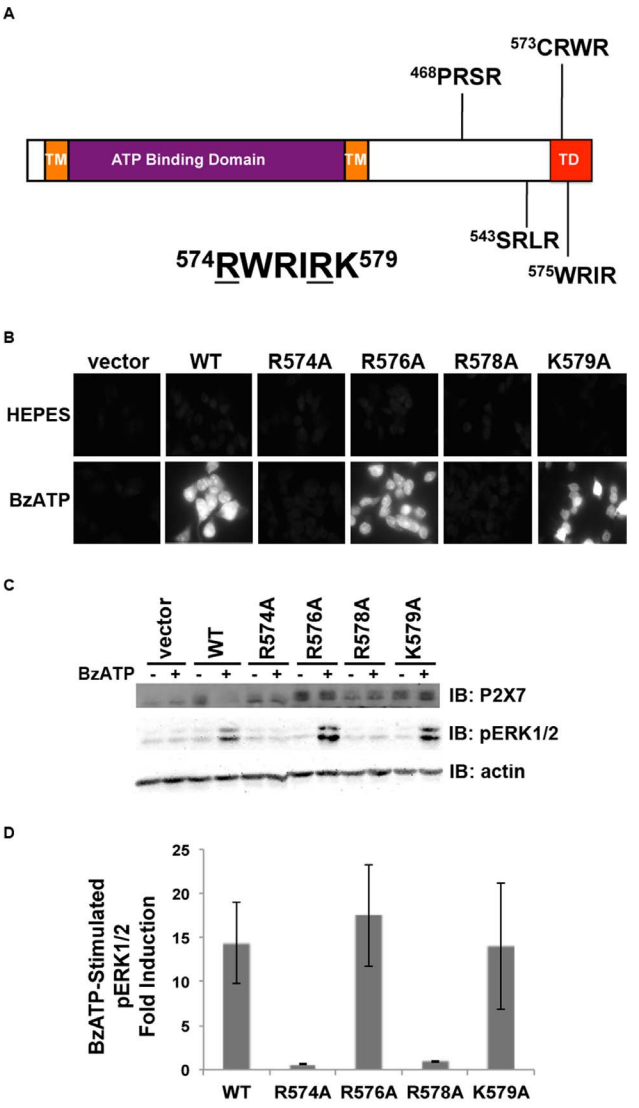

Figure 1. Amino acids Arg574 and Arg578 within the trafficking domain (and potential ER retention sequences) are critical for $P2X_7$ activity. A, Human $P2X_7$ contains two transmembrane domains, an extracellular ATP binding domain, and an intracellular C-terminal domain containing a region important for cell surface localization (TD). The receptor also contains four potential Arg-X-Arg ER retention sequences beginning at amino acids 468, 543, 573 and 575 [18]. The underlined amino acids were found to be important for $P2X_7$ activity. TM = transmembrane domain, TD = trafficking domain. **B,** HEK293 cells expressing $P2X_7$ R574A or R578A but not the R576A or K579A mutants exhibit attenuated BzATP-stimulated pore formation. Cells were treated for 10 min with 250 μM BzATP in the presence of the fluorescent dye YO-PRO-1. The pores were closed by the addition of $MgCl_2$, and the cells were imaged for relative YO-PRO-1 uptake. These data are representative of at least four experiments. **C and D,** The $P2X_7$ R574 and R578 mutants but not the R576A and K579A mutants have an attenuated ability to activate ERK1/2 upon nucleotide stimulation. The lower band observed in every lane on the $P2X_7$ immunoblot is a non-specific protein; the top band is exogenous $P2X_7$. The error bars represent the standard error of the mean. These data are representative of at least three experiments.
doi:10.1371/journal.pone.0063789.g001

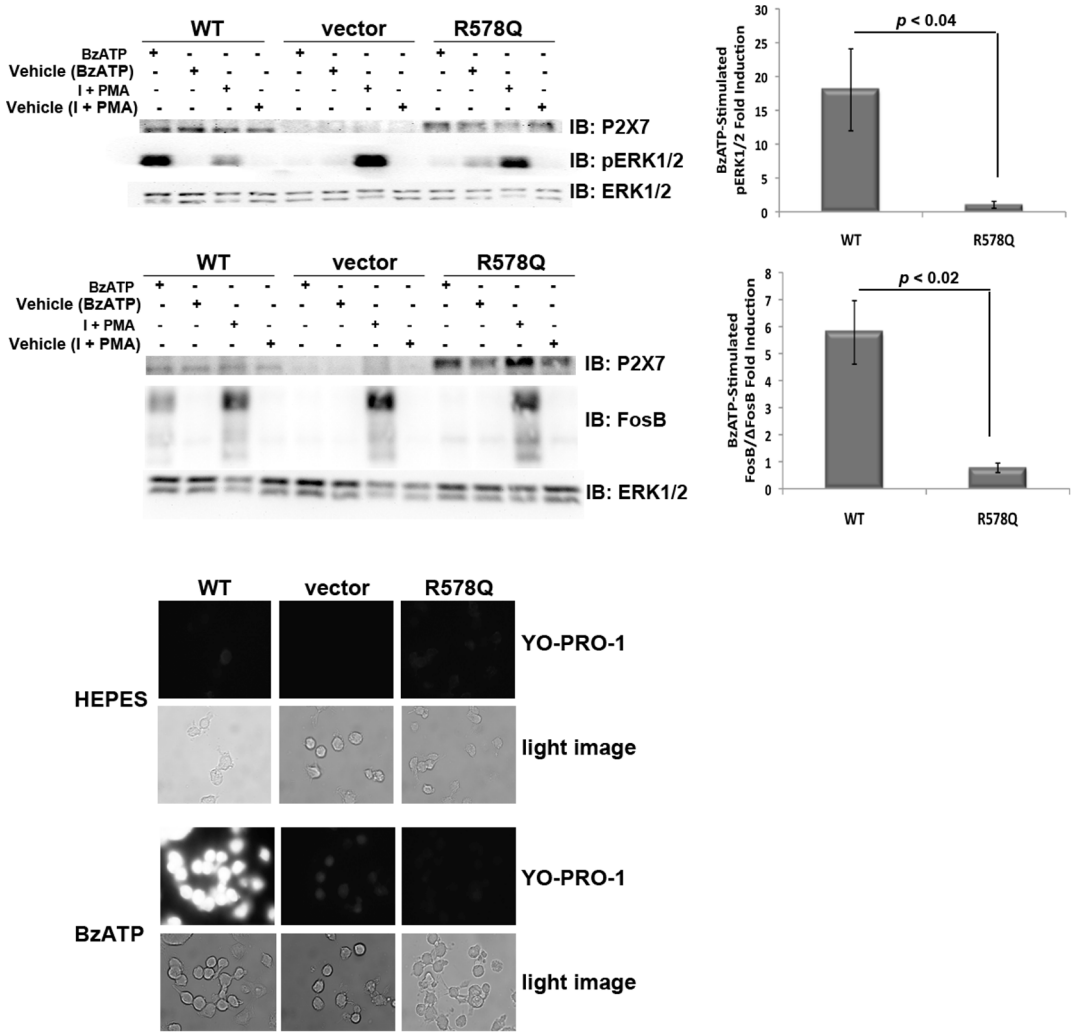

Figure 2. The P2X$_7$ R578Q variant exhibits attenuated nucleotide-stimulated signaling and pore formation. A and B, HEK293 cells expressing the P2X$_7$ R578Q variant exhibit attenuated ERK1/2 activation. We have previously found that treatment with 1 μg/mL PMA plus 1 μg/mL ionomycin promotes ERK1/2 activation (data not shown), and this co-treatment was used here as a positive control. The error bars represent the standard error of the mean. These data are representative of at least three experiments. **C and D,** HEK293 cells expressing the P2X$_7$ R578Q variant display decreased nucleotide-induced FosB/ΔFosB induction in comparison to wild-type P2X$_7$. We have previously found that treatment with 1 μg/mL PMA plus 1 μg/mL ionomycin stimulates FosB/ΔFosB induction (data not shown), and this co-treatment was used here as a positive control. The top band on the FosB immunoblot is full-length FosB and the lower bands are its truncated splice variant ΔFosB [27]. The error bars represent the standard error of the mean. These data are representative of at least three experiments. **E,** The P2X$_7$ R578Q variant displays drastically attenuated pore formation. These images are representative of at least three experiments. I = ionomycin.
doi:10.1371/journal.pone.0063789.g002

statistical significance between the normalized levels of the P2X7$_7$ wild-type and P2X$_7$ R578Q trimers.

Flow Cytometry

HEK293 stable cell lines were cultured in 10 cm plates to subconfluency. The cells were lifted by brief exposure with 0.25% trypsin, pelleted at 200×*g*, and suspended in 1X PBS pH 7.4 containing 1% CCS. 5×10^5 cells were treated with 1 μg/μl anti-P2X$_7$ or 1 μg/μl IgG2b isotype control for 30 min at 4°C. The cells were washed with 1 mL of 1% CCS PBS and suspended in 100 μl 1% CCS PBS. Secondary labeling of cells was performed with 1 μg/μl Alexa Fluor 488-conjugated goat anti-mouse IgG for 30 min at 4°C. After an additional wash, the cells were suspended in 200 μl 1% CCS PBS. To exclude dead cells, 3 μg/ml propidium iodide was added to each sample. A total of 10,000 events were collected on a FACSCalibur flow cytometer (BD Biosciences) at the University of Wisconsin Carbone Cancer Center Flow Cytometry Core Facility. The data were analyzed with FlowJo analysis software (TreeStar, OR).

Cell Viability Assay

HEK293 stable cell lines that were treated with BS^3, DSS or tunicamycin were incubated with 0.2% trypan blue and visualized by microscopy. All of the cells in one field of view (~70 cells) were counted, the number of trypan blue-positive cells was determined, and the percent viability was calculated.

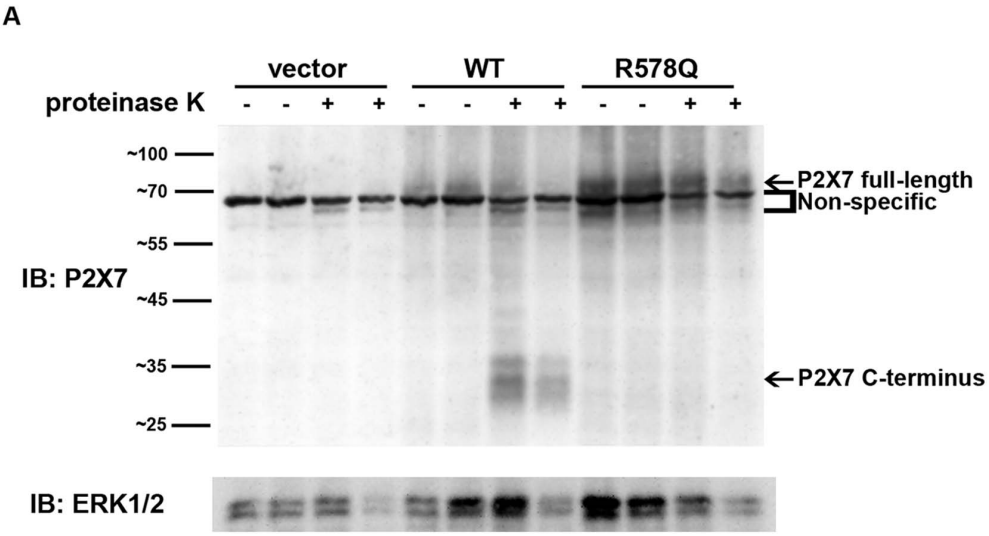
A
vector
WT
R578Q
proteinase K
- - + + - - + + - - + +
~100
~70
~55
~45
~35
~25
IB: P2X7
P2X7 full-length
Non-specific
P2X7 C-terminus
IB: ERK1/2

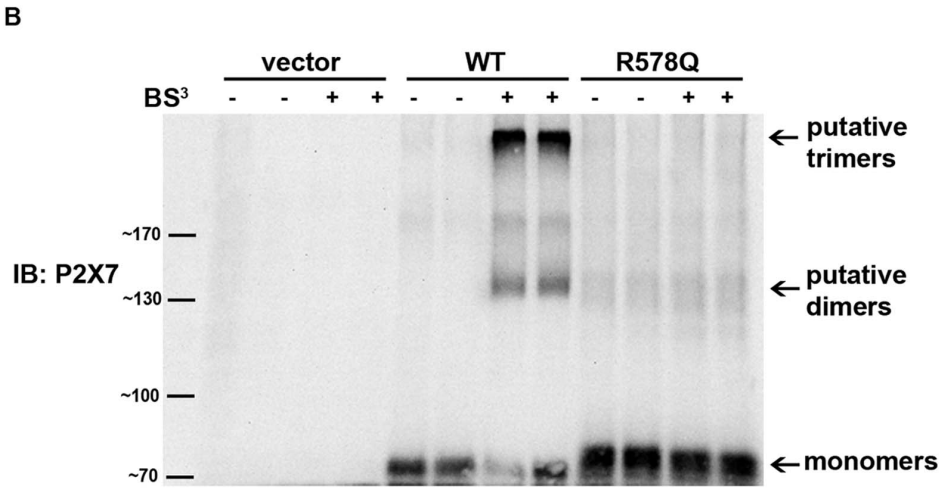
B
vector
WT
R578Q
BS3
- - + + - - + + - - + +
~170
~130
~100
~70
IB: P2X7
putative trimers
putative dimers
monomers

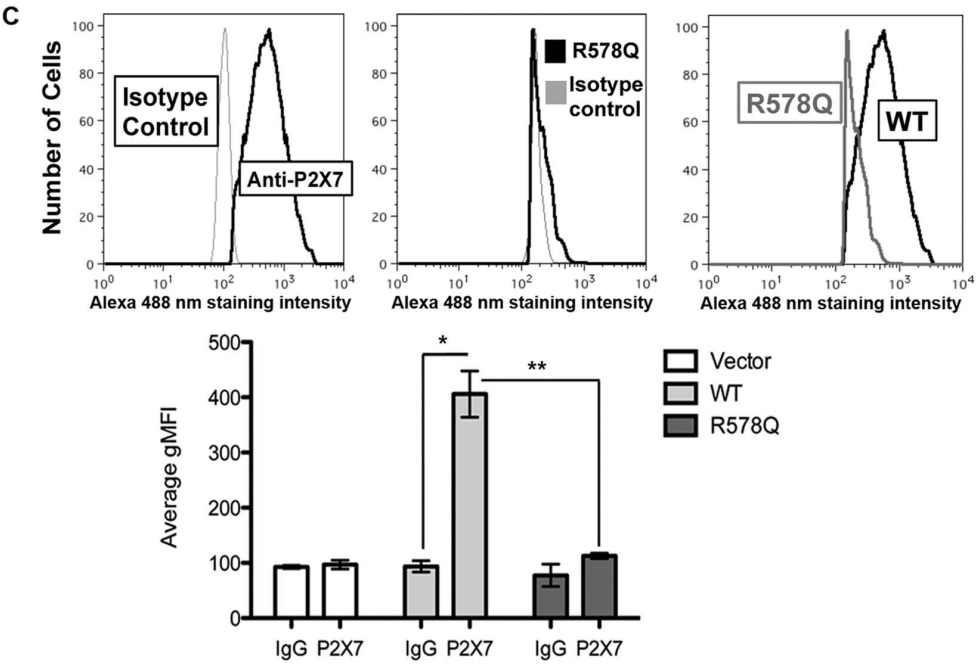
C
Number of Cells
Isotype Control
Anti-P2X7
R578Q
Isotype control
R578Q
WT
Alexa 488 nm staining intensity
Alexa 488 nm staining intensity
Alexa 488 nm staining intensity
Average gMFI
*
**
Vector
WT
R578Q
IgG P2X7 IgG P2X7 IgG P2X7

Figure 3. $P2X_7$ R578Q is not expressed on the plasma membrane. A, HEK293 stable cell lines were treated with the broad-spectrum protease proteinase K to detect the presence of the ~30 kDa $P2X_7$ C-terminal tail that is liberated when the extracellular domain of $P2X_7$ is digested by protease when the receptor is localized at the plasma membrane. These data are representative of three experiments. **B,** HEK293 stable cell lines were treated with the cell-impermeable chemical cross-linker BS^3 to detect $P2X_7$ localization at the cell surface. The $P2X_7$ monomers and putative dimers and trimers are indicated. The predicted molecular weight of human $P2X_7$ is ~69 kDa and it contains several N-linked glycosylation sites that result in slower mobility in SDS-PAGE gels [15]. Thus, $P2X_7$ dimers are predicted to exhibit an apparent mass slightly greater than 140 kDa and $P2X_7$ trimers are predicted to exhibit an apparent mass slightly greater than 210 kDa. These data are representative of at least four experiments. **C,** HEK293 cells were stained with an anti-$P2X_7$ antibody or IgG isotype control, and the relative levels of surface-exposed $P2X_7$ WT and R578Q were determined by flow cytometry. The graph represents the average of three independent experiments. * $p<0.006$, ** $p<0.007$. gMFI = geometric mean fluorescence intensity.
doi:10.1371/journal.pone.0063789.g003

Endo H glycosidase Assay

HEK293 stable cell lines were harvested in 2X sample buffer, and the proteins were denatured by boiling for 10 min. The cell lysates were typically treated with 5 U EndoH in 50 mM sodium citrate (pH 5.5) at 37°C for 1 h. The proteins (~50 μg) were then resolved on 12.5% polyacrylamide gels containing SDS, transferred to PVDF membranes, and immunoblotted with an anti-$P2X_7$ antibody.

Tunicamycin Assay

HEK293 stable cell lines were pretreated with 1 μg/ml of tunicamycin for approximately 48 h and then incubated with 500 μM DSS for 15 min prior to quenching by the addition of 20 mM Tris HCl pH 7.5. The cells were harvested in 2X sample buffer, sonicated, boiled and immunoblotted as described above. To compare the relative levels of trimers that formed with and without tunicamycin treatment, Adobe Photoshop CS4 Version 11.0 was used to obtain the relative band intensities of the $P2X_7$ monomers, $P2X_7$ trimers, and vinculin (loading control). The $P2X_7$ trimer values were normalized to the relative expression levels of the monomers, and the adjusted values for the $P2X_7$ trimers were then normalized to vinculin.

Results

$P2X_7$ amino Acids Arg 574 and Arg 578 within the Trafficking Domain are Critical for Receptor Activity

We previously demonstrated that the distal C-terminus of human $P2X_7$ is critical for its activity and localization at the plasma membrane [10]. Specifically, we generated the $P2X_7$ R578E/K579E double mutant to investigate its conserved lipopolysaccharide (LPS) binding domain and found that mutation of R578 and K579 results in attenuated $P2X_7$-stimulated ion currents, pore formation and apoptosis [8,10]. We analyzed the sequence of the intracellular C-terminus to identify motifs that may regulate trafficking and found that $P2X_7$ contains four RXR sequences, motifs for the poorly understood Arg-based ER retention signals (Fig. 1a). Arg-based ER retention signals reportedly conform to the sequence Φ/Ψ/R-R-X-R where Φ/Ψ represents an aromatic or bulky hydrophobic residue and X is any amino acid [18]. We previously postulated that human $P2X_7$ contains an Arg-based ER retention sequence at amino acids 576–578 and demonstrated that double mutation of R576 and R578 to Ala results in attenuated $P2X_7$ ligand-stimulated pore formation [6]. Here we sought to determine which specific residues in the Arg-X-Arg sequences within the trafficking domain modulate $P2X_7$ function. We tested the ability of alanine substitutions to stimulate $P2X_7$ ligand-induced pore formation and ERK1/2 activation. As shown in Figure 1, mutation of R574 or R578 but not mutation of R576 or K579 results in attenuated BzATP-stimulated pore formation and ERK1/2 phosphorylation/activation. These results indicate that R574 and R578 but not R576 and K579 are important for $P2X_7$ activity.

The $P2X_7$ Arg578 to Gln Polymorphism Exhibits Attenuated BzATP-induced Signaling and Pore Formation

To determine whether a naturally-occurring variant within the $P2X_7$ trafficking domain exhibits attenuated activity, we examined BzATP-stimulated ERK1/2 phosphorylation/activation, FosB/ΔFosB induction, and pore formation in HEK293 cells stably-expressing $P2X_7$ R578Q [6,12,15]. The $P2X_7$ R578Q mutation is more structurally similar to Arg compared to Ala. As shown in Figure 2, mutation of R578 to Gln results in attenuation of both signaling (ERK1/2 phosphorylation/activation and FosB/ΔFosB induction) and pore activity. The R578Q variant resulted in approximately a 17-fold reduction in ERK1/2 activation and approximately a 6-fold reduction in FosB/ΔFosB induction in comparison to $P2X_7$ wild-type. The cells were treated with PMA and ionomycin as a positive control to verify that introduction of $P2X_7$ R578Q does not result in a global inability to activate ERK1/2 or induce FosB/ΔFosB. It is worth noting that throughout our studies the relative expression levels between $P2X_7$ wild-type and the R578Q mutant were typically within a 1.5 to 2-fold difference. These results show that a $P2X_7$ distal C-terminal variant found in the human population also displays reduced receptor function.

$P2X_7$ R578Q does not Stably Express on the Cell Surface

To assess the mechanism by which $P2X_7$ R578Q exhibits reduced function, we used a protease digestion assay that we previously developed [15] to demonstrate that there is no detectable $P2X_7$ R578Q expressed on the plasma membrane (Figure 3a). In this assay, live cells are exposed to the broad-spectrum protease proteinase K for a given period of time. The extracellular domain of $P2X_7$ is digested by protease when the receptor is localized at the plasma membrane, liberating the intracellular C-terminal tail that can be detected by immunoblotting using antibodies raised against the C-terminus. The data in Figure 3a demonstrate that the $P2X_7$ R578Q polymorphism exhibits a drastically reduced ability to properly localize.

To further verify that $P2X_7$ R578Q does not stably express at the plasma membrane, we used a chemical cross-linker to examine the presence of $P2X_7$ trimers at the cell surface. Intact cells were treated with BS^3, a hydrophilic, cell impermeable, non-cleavable cross-linker [19], and the presence of $P2X_7$ trimers was assess by immunoblotting. Many groups have reported that $P2X_7$ exists as a homotrimer [4,17,20–22]. As shown in Figure 3b, cross-linking proteins on live cells promotes the detection of putative $P2X_7$ wild-type trimers but not the detection of $P2X_7$ R578Q oligomers. The mass of the multimeric complex for wild-type $P2X_7$ is consistent with $P2X_7$ homotrimer formation (Figure 4g).

We also utilized flow cytometry to demonstrate that $P2X_7$ wild-type but not $P2X_7$ R578Q is expressed on the plasma membrane of HEK293 cells (Fig. 3c). There was a statistically significant difference in the amount of wild-type receptor observed at the cell

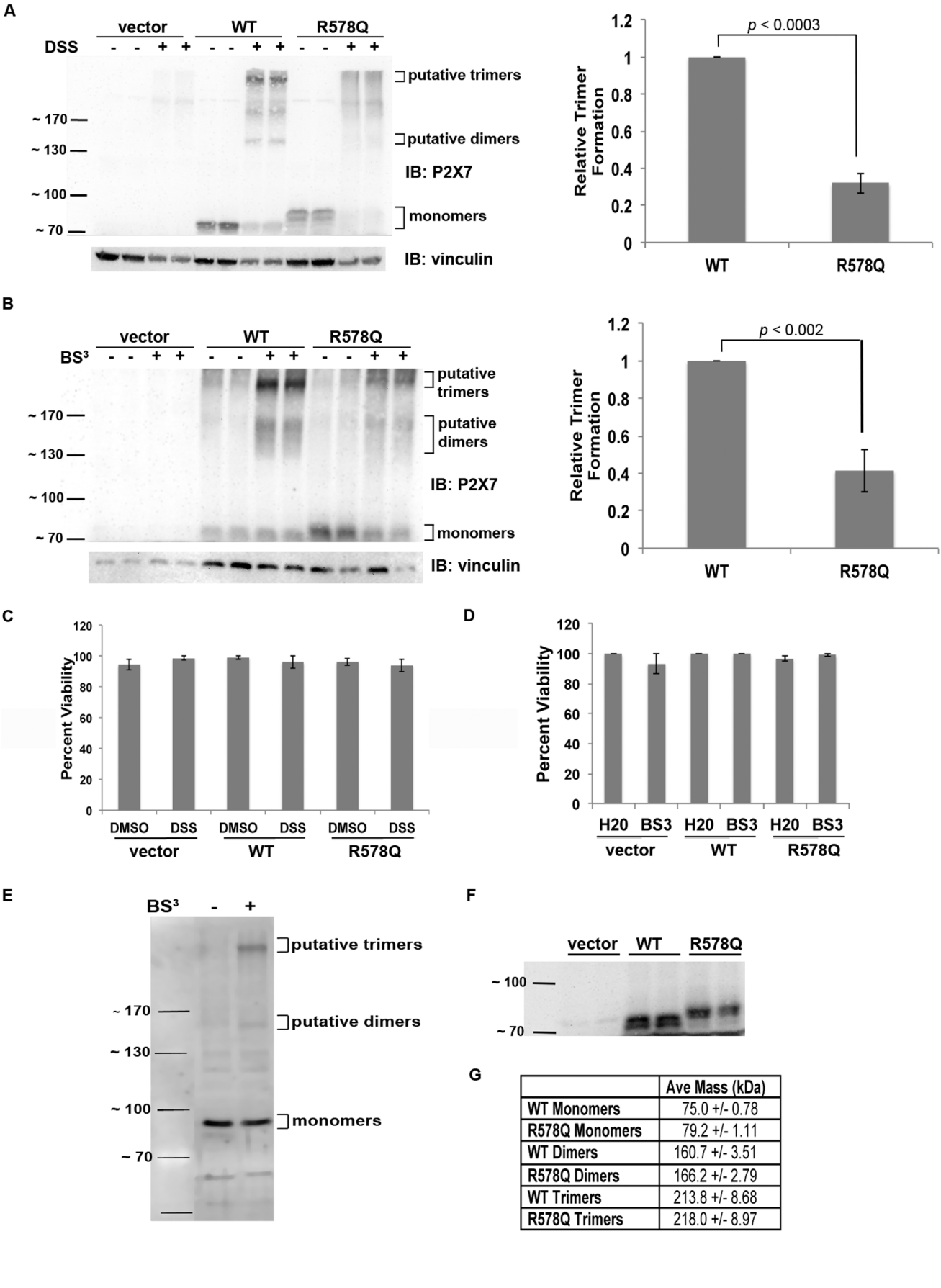

	Ave Mass (kDa)
WT Monomers	75.0 +/- 0.78
R578Q Monomers	79.2 +/- 1.11
WT Dimers	160.7 +/- 3.51
R578Q Dimers	166.2 +/- 2.79
WT Trimers	213.8 +/- 8.68
R578Q Trimers	218.0 +/- 8.97

Figure 4. $P2X_7$ R578Q displays defective oligomerization. A, HEK293 cells were treated with the cell-permeable chemical cross-linker DSS to demonstrate that intracellular $P2X_7$ R578Q does not oligomerize as efficiently as wild-type receptor. The samples were blotted with anti-vinculin antibody as a loading control. The average difference in the amount of $P2X_7$ wild-type trimers that formed following treatment with DSS was calculated and compared to the amount of $P2X_7$ R578Q trimers that formed. A Student's *t*-test was performed to determine statistical significance. These data are representative of five experiments. **B,** Proteins from HEK293 lysates were cross-linked with BS^3, and the difference in the amount of $P2X_7$ wild-type trimers that formed upon cross-linking with BS^3 was compared to the amount of $P2X_7$ R578Q trimers that formed. A Student's *t*-test was performed to determine statistical significance. These data are representative of five experiments. **C,D,** HEK293 cells were incubated in the presence of DSS or BS^3, respectively, or the appropriate vehicle control. The cells were stained with trypan blue and counted to determine the percent viability. The error bars represent the standard error of the mean. These data are representative of three experiments. **E,** Human monocytes were treated with BS^3 to demonstrate that upon cross-linking, endogenous $P2X_7$ displays a banding pattern that is consistent with dimer and trimer formation. These data are representative of four experiments. **F,** Proteins from untreated lysates were resolved on 12.5% SDS-polyacrylamide gels to demonstrate the apparent size difference between $P2X_7$ wild-type and R578Q. These data are representative of at least fifteen experiments. **G,** The molecular masses of the $P2X_7$ wild-type and R578Q monomers and their putative dimers and trimers were extrapolated using the distance the molecular weight standards migrated. The results were averaged and the standard error of the mean was determined. Seven replicates were used to calculate the average mass of the monomers, and three replicates were used to calculate the mass of the dimers and trimers.
doi:10.1371/journal.pone.0063789.g004

surface in comparison to the amount of the R578Q variation present ($p<0.007$). In addition to demonstrating that $P2X_7$ R578Q trimers are not stably expressed at the cell surface, these results demonstrate that wild-type $P2X_7$ constitutively exists as a trimer at the plasma membrane and does not require ligand stimulation to oligomerize.

The $P2X_7$ R578Q SNP Displays Defective Oligomerization

To further delineate the mechanism by which $P2X_7$ R578Q possesses reduced function, we tested the idea that this mutant displays defective oligomerization. We cross-linked proteins from both live cells and cell lysates and demonstrate that R578Q does not oligomerize as efficiently as wild-type receptor (Fig. 4). In Figure 4a, we treated live cells with the cell permeable cross-linker DSS and observed that treatment with DSS results in the formation of less $P2X_7$ R578Q trimers in comparison to wild-type ($p<0.0003$). To validate these results, cell lysates were treated with BS^3 (Fig. 4b). As with the live cells, we observed that the R578Q variant forms less trimers upon cross-linking in comparison to wild-type receptor ($p<0.002$). Thus, we have presented evidence that the $P2X_7$ R578Q mutant does not exist as a trimeric complex at the cell surface (Fig. 3b), a significantly larger portion of intracellular $P2X_7$ wild-type receptor exists as trimers in comparison to intracellular $P2X_7$ R578Q trimers (Fig. 4a), and the total amount of wild-type receptor that oligomerizes is greater than the total amount of $P2X_7$ R578Q that oligomerizes (Fig. 4b).

To examine the possibility that treatment with the chemical cross-linkers induces cell death and potential protein-protein interactions that do not occur in normal, intact healthy cells, we performed cell viability assays. As shown in Figures 4c and 4d, there was no observable cell death that occurs in the presence of DSS or BS^3, respectively.

To further support our interpretation that the ~210 kDa bands observed upon cross-linking HEK293 cells are $P2X_7$ trimers, we cross-linked proteins from human monocytes and observed that endogenous $P2X_7$ also appears to trimerize upon treatment with BS^3 (Fig. 4e).

In addition, we observed that when $P2X_7$ wild-type and the R578Q mutant are resolved on 12.5% polyacrylamide gels, it becomes more apparent that the R578Q monomers migrate slower than wild-type protein (Fig. 4f). This suggests that $P2X_7$ R578Q may contain a larger mass of post-translational modifications than wild-type $P2X_7$. We used the molecular weight standards to extrapolate the masses of the monomers, dimers, and trimers of $P2X_7$ wild-type and $P2X_7$ R578Q (Fig. 4g). As predicted, the monomers of both $P2X_7$ wild-type and R578Q exhibited an apparent molecular weight greater than the calculated weight of 69 kDa (no post-translational modifications), the dimers have an apparent weight greater than 140 kDa, and the trimers have an apparent mass that is greater than 210 kDa. Interestingly, the monomers, dimers, and trimers of the $P2X_7$ R578Q mutant have a higher calculated mass than the monomers, dimers, and trimers of wild-type receptor.

$P2X_7$ R578Q is More Heavily Glycosylated than Wild-type $P2X_7$

To test the hypothesis that the R578Q mutant possesses a larger mass of N-linked glycosylation modifications, we compared the relative molecular masses of $P2X_7$ wild-type and R578Q both before and after deglycosylation by Endo H. We previously reported that $P2X_7$ is N-linked glycosylated on N187, N202, N213, N241 and N284 [15]. As shown in Figures 4f and 5, wild-type $P2X_7$ migrates faster than the R578Q mutant. Based upon SDS-PAGE gel analysis, treatment with Endo H results in a decrease in mass, and the molecular masses of $P2X_7$ wild-type and the R578Q variant are approximately the same following deglycosylation (Fig. 5a). The molecular mass of $P2X_7$ wild-type and the R578Q variant both before and after deglycosylation were calculated and compared (Fig. 5b). There was a statistically significant difference in the sizes of the untreated receptors, but there was no apparent difference in the size of the receptors that were deglycosylated with Endo H. The mass of $P2X_7$ wild-type was calculated to be 75.0 kDa and the mass of $P2X_7$ R578Q was calculated to be 79.2 kDa. The difference in mass between deglycosylated wild-type and deglycosylated mutant receptor is drastically smaller; deglycosylated wild-type $P2X_7$ has a calculated mass of 53.3 kDa while $P2X_7$ R578Q has a calculated mass of 53.8 kDa. Of note, human $P2X_7$ without any post-translational modifications has a predicted molecular mass of approximately 69 kDa, but upon deglycosylation the protein may be folded in a manner that allows faster migration through SDS-PAGE gels, causing the receptor to migrate at approximately the same position as the 55 kDa standard [15].

N-linked Glycosylation and Oligomerization of $P2X_7$ are Independent Events

To determine the significance of N-linked glycosylation in $P2X_7$ oligomerization, we inhibited N-linked glycosylation via treatment with tunicamycin and assessed the ability of $P2X_7$ wild-type to cross-link (Fig. 6). Because fewer $P2X_7$ monomers and $P2X_7$ trimers were observed following tunicamycin treatment (Fig. 6a), we performed cell viability assays to assess whether tunicamycin induces cell death (Fig. 6b). Cells treated with 1 μg/ml tunicamycin or methanol vehicle control for 48 h exhibited little difference in cell viability. Thus, the differences in trimer formation with or without tunicamycin were normalized to the

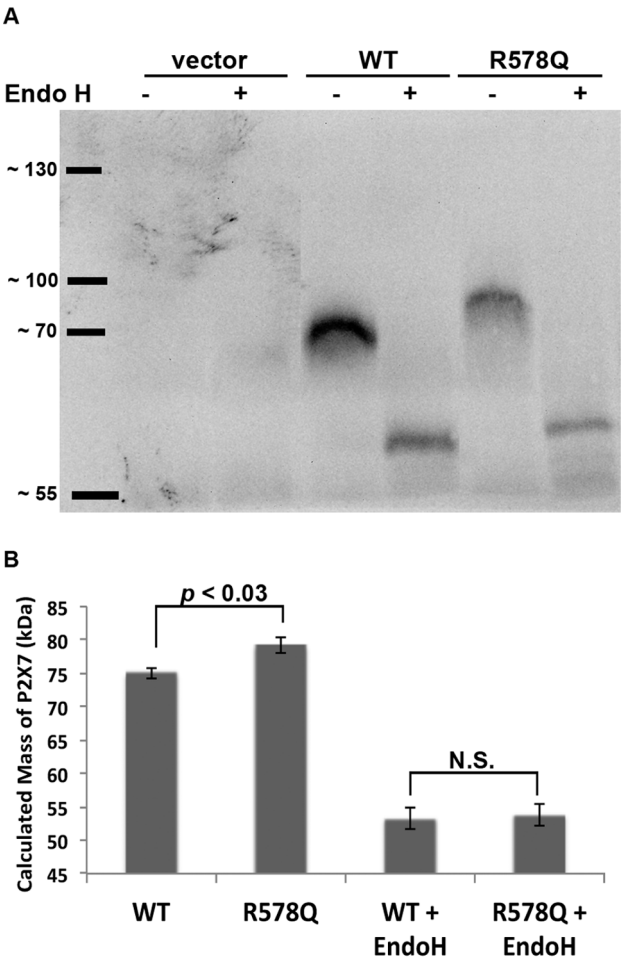

Figure 5. P2X$_7$ R578Q contains a larger mass of N-linked glycosylation modifications than wild-type receptor. A, Proteins from cell lysates were treated with the glycosidase Endo H and compared with the mobility of proteins from untreated lysates. The size difference between glycosylated P2X$_7$ wild-type and P2X$_7$ R578Q appears to be larger than the size difference between the deglycosylated receptors. These data are representative of three experiments. **B,** The molecular mass of untreated and Endo H-treated P2X$_7$ wild-type and P2X$_7$ R578Q were calculated using the distance the molecular weight standards migrated. The error bars represent the standard error of the mean. Seven replicates were used to calculate the mass of untreated P2X$_7$, and three replicates were used to calculate the mass of Endo H-treated P2X$_7$. N.S. = not statistically significant.
doi:10.1371/journal.pone.0063789.g005

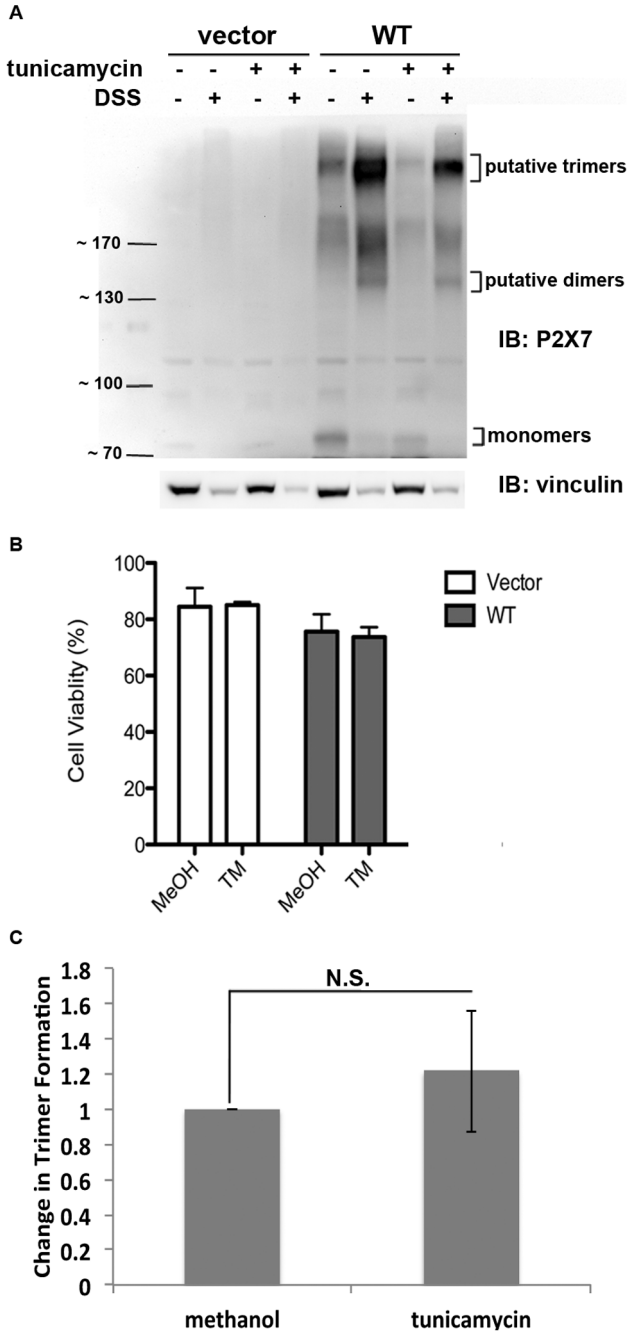

Figure 6. Oligomerization of P2X$_7$ is independent of glycosylation. A, Protein was cross-linked following treatment with the N-linked glycosylation inhibitor tunicamycin and immunoblotted to detect the formation of P2X$_7$ wild-type trimers. **B,** A cell viability assay was performed to determined whether tunicamycin induces cell death. These data are the average of three independent experiments, and the error bars represent the standard error of the mean. MeOH = methanol, TM = tunicamycin. **C,** The results were quantified as described above and indicate that there was no observable difference in the amount of trimers that formed with or without tunicamycin. These data represent the average of five independent experiments. N.S. = not statistically significant.
doi:10.1371/journal.pone.0063789.g006

relative levels of monomers that were observed following treatment with methanol or tunicamycin for 48 h (Fig. 6c). Student's *t*-tests were performed to determine whether there were statistically significant differences, and no differences were observed ($p = 0.57$). Thus, after normalizing the levels of P2X$_7$ trimers to the amount of monomers present, treatment with tunicamycin for 48 h does not appear to attenuate the ability of P2X$_7$ to oligomerize.

Alanine Mutations within the Arg-X-Arg Sequences Located at Amino Acids 469 and 544 do not Result in Altered P2X$_7$ Activity

To determine whether the RXR sequences located at amino acids R469 and R544 are also important for receptor activity (Fig. 1a), we generated alanine substitutions at these motifs and assessed BzATP-stimulated pore formation and cell signaling. As shown in Figure 7, P2X$_7$ R469A/R471A and P2X$_7$ R544A both exhibit BzATP-stimulated pore formation, FosB/ΔFosB induction and ERK1/2 phosphorylation/activation that is similar to that

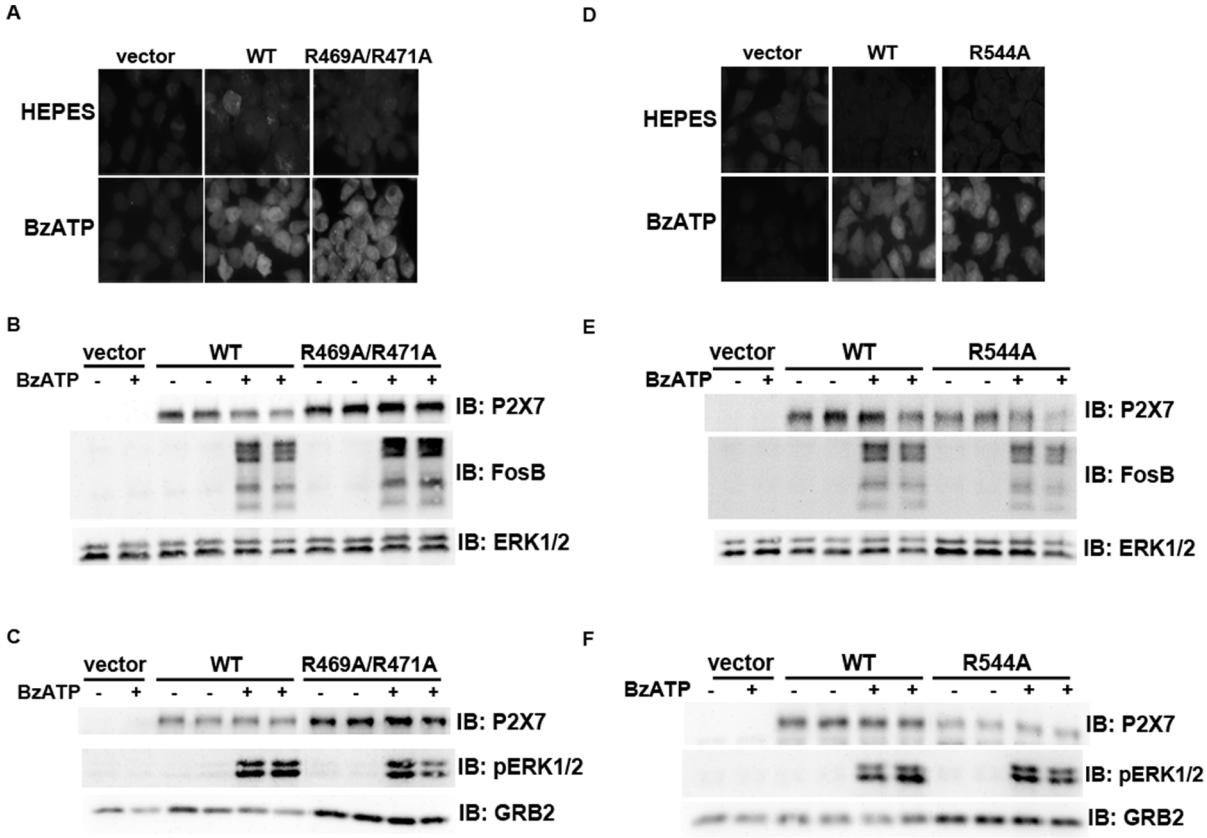

Figure 7. Mutations within the other Arg-X-Arg sequences do not result in altered $P2X_7$ activity. A and D, The $P2X_7$ R469A/R471A double mutant and the $P2X_7$ R554A single mutant do not display attenuated nucleotide-stimulated pore activity. These data are representative of at least three experiments. **B and E,** The $P2X_7$ R469A/R471A and R554A mutants do not display attenuated BzATP-stimulated FosB/ΔFosB induction. The anti-FosB antibody recognizes both full-length FosB (indicated by the top three bands) and its truncated splice variant ΔFosB (indicated by the bottom two bands). These data are representative of at least two experiments. **C and F,** The $P2X_7$ R469A/R471A and R554A mutants exhibit normal nucleotide-stimulated ERK1/2 activation. These data are representative of two experiments.
doi:10.1371/journal.pone.0063789.g007

observed for wild-type $P2X_7$. The fold changes in FosB/ΔFosB induction and ERK1/2 activation by $P2X_7$ wild-type, R469A/R471A and R544A were calculated and compared. The differences in FosB/ΔFosB induction between $P2X_7$ wild-type and $P2X_7$ R469A/R571A differed within 1.5 fold, and the differences between $P2X_7$ wild-type and R544A differed within 1.3 fold. As for pERK1/2 activation, the differences between wild-type and R469A/R471A differed within 1.7 fold and 1.5 for wild-type and R544A.

Discussion

We present evidence that residue R578 in human $P2X_7$ is important for processing newly synthesized $P2X_7$ in the ER where N-linked glycosylation addition/trimming and oligomerization occurs [23]. Although we and other groups have demonstrated that mutations in the distal C-terminus of $P2X_7$ result in attenuated activity and cell surface presentation [6,7,9,11], this is the first report to our knowledge that describes a possible mechanism by which amino acid changes in this region result in reduced function. Our data indicate there is an apparent size difference between wild-type $P2X_7$ and the R578Q variant, and this mass difference is attributed in part to the presence of increased oligosaccharides on the R578Q mutant. This result supports the idea that mutation of R578 prevents the proper addition and/or trimming of N-linked glycosylation modifications, due to defective $P2X_7$ processing in the ER [23].

$P2X_7$ contains the sequence encoding an Arg-based ER retention signal beginning at amino acid W575 that conforms to the sequence Φ/Ψ/R-R-X-R where Φ/Ψ represents an aromatic or bulky hydrophobic residue and X is any amino acid (Fig. 1a and [18]). Our data demonstrating that mutation of R578 results in reduced activity and impaired oligomerization and modification of N-linked glycosylation is supportive of the idea that $P2X_7$ R578Q has an ER protein processing defect. One potential explanation for why mutation of R578 attenuates $P2X_7$ activity is that disruption of the R-X-R sequence restricts ER retention, causing $P2X_7$ to traffic through the ER before it is properly oligomerized and its N-linked glycans are processed by N-glycan-modifying enzymes. We present several data that indicate $P2X_7$ oligomerizes in the secretory pathway and is trafficked to the plasma membrane as a trimer: 1) $P2X_7$ trimers are detected on the plasma membrane even in the absence of ligand stimulation (Fig. 3b) and 2) cell-permeable DSS cross-links $P2X_7$ monomers (Figs. 4a and 6). There are numerous reports of plasma membrane-bound receptors oligomerizing in the ER [24,25]. Thus, we propose that both the oligomerization and N-linked glycosylation defects observed for $P2X_7$ are attributed to inefficient processing in the ER (Fig. 8). As shown in Figure 6, oligomerization of $P2X_7$ appears to be independent of N-linked glycosylation, thus the defect in N-linked

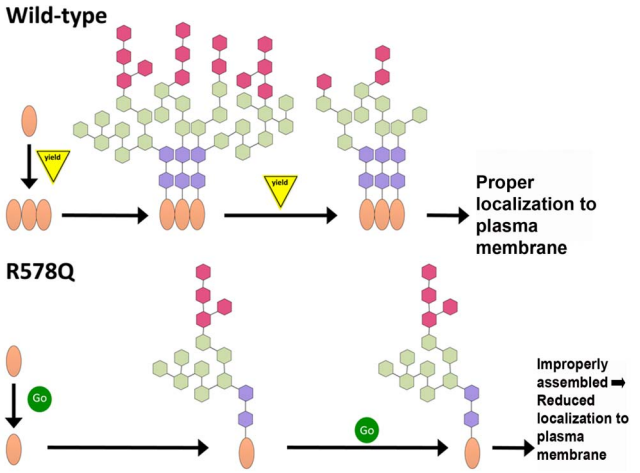

Figure 8. Model of wild-type and mutant $P2X_7$ assembly. We propose that $P2X_7$ is synthesized in the ER where it is oligomerized and its N-linked glycosylation modifications are added. Mutation of the trafficking domain results in altered kinetics through the secretory pathway, leading to faulty trimerization and insufficient trimming of N-linked glycosylation modifications. Improperly assembled $P2X_7$ either does not traffic to the plasma membrane or is quickly removed after it is localized at the plasma membrane. In the model, the protein monomers are indicated by an oval, and the sugar groups are represented by the colored hexagons.
doi:10.1371/journal.pone.0063789.g008

glycosylation addition/trimming likely does not contribute to the defect in the ability of $P2X_7$ R578Q to trimerize. We postulate that the rate by which $P2X_7$ R578Q travels through the ER is altered, potentially through a retention defect, contributing to both the oligomerization and glycosylation problems (Fig. 8).

In contrast to the idea that $P2X_7$ contains an R-X-R ER retention signal, mutation of R576 within the Φ/Ψ/R-R-X-R sequence did not result in reduced activity while mutation of R574 attenuated $P2X_7$ signaling and pore formation (Fig. 1). These data indicate that if $P2X_7$ contains an Arg-based ER retention signal, it does not conform to the Φ/Ψ/R-R-X-R sequence. An alternative explanation to ER retention is that R574 and R578 belong to an ER exit motif. Mutation of R578 to glutamine may prevent $P2X_7$ from entering the golgi, allowing for the excessive addition of N-glycans that cannot be trimmed by N-glycan modifying enzymes found later in the secretory pathway. Based on the data presented, we cannot rule out the possibility that oligomerization occurs in the golgi and thus R578 may belong to an ER exit motif.

Because a large portion of $P2X_7$ wild-type and R578Q are localized in the ER, as evident by their sensitivity to Endo H (Fig. 5), it is difficult to identify the stage in the secretory pathway where the R578Q defect is occurring. More studies are required to determine whether $P2X_7$ R578Q exhibits an ER retention and/or ER exit defect and if its trafficking kinetics through the secretory pathway are indeed altered. A detailed analysis will be needed to identify the specific stage in the pathway where the R578Q variant exhibits its defect. Nonetheless, this investigation demonstrates that the distal C-terminus is critical for normal $P2X_7$ activity and that mutation of this region causes decreased receptor function through defective N-linked glycosylation processing, oligomerization, and trafficking to and/or from the plasma membrane.

Our tunicamycin studies revealed the interesting finding that the basal state levels of $P2X_7$ monomers are regulated by an N-linked glycosylation-dependent mechanism. As observed in Figure 6, treatment with tunicamycin reduces $P2X_7$ protein levels although the cell viability values are similar for cells treated with vehicle, and tunicamycin does not appear to reduce the levels of the loading control vinculin. Thus, it is possible that $P2X_7$ synthesis and/or stability are regulated by a protein(s) that is N-linked glycosylated. It would be interesting to characterize the signaling networks that regulate $P2X_7$ transcription and protein turnover as this has been largely unexplored. A recent report has shown that the Specificity protein 1 (Sp1) transcription factor regulates $P2X_7$ levels in primary cortical neurons and astrocytes [26].

In summary, we provide evidence that human $P2X_7$ residues R574 and R578 are required for BzATP-stimulated signaling and pore formation, and that the mutation of R578 to glutamine results in impaired oligomerization and the improper addition and/or trimming of N-linked glycosylation modifications, indicative of a potential processing defect in the ER. To our knowledge, these data are the first to help define the mechanism by which the $P2X_7$ distal C-terminus contributes to normal receptor function.

Acknowledgments

The authors thank Dr. Judy Smith for helpful discussions and Drs. Colleen Curran, Monica Gavala and David Manthei for critically reviewing this manuscript.

Author Contributions

Conceived and designed the experiments: LYL JBB LEW PJB. Performed the experiments: LYL JBB LEW NVW. Analyzed the data: LYL JBB LEW PJB JMD LCD NVW. Contributed reagents/materials/analysis tools: PJB JMD LCD. Wrote the paper: LYL. Helped with revising the manuscript: JMD LCD LEW JBB.

References

1. Romagnoli R, Baraldi P, Cruz-Lopez O, Lopez-Cara C, Preti D, et al. (2008) The P2X7 receptor as a therapeutic target. Expert Opin Ther Targets 12: 647–661.
2. Lenertz LY, Gavala ML, Zhu Y, Bertics PJ (2011) Transcriptional control mechanisms associated with the nucleotide receptor P2X7, a critical regulator of immunologic, osteogenic, and neurologic functions. Immunol Res 50: 22–38.
3. Gunosewoyo H, Kassiou M (2010) P2X purinergic receptor ligands: recently patented compounds. Expert Opin Ther Pat 20: 625–646.
4. North R (2002) Molecular physiology of P2X receptors. Physiol Rev 82: 1013–1067.
5. Lazarowski ER, Boucher RC, Harden TK (2003) Mechanisms of release of nucleotides and integration of their action as P2X- and P2Y-receptor activating molecules. Mol Pharmacol 64: 785–795.
6. Lenertz L, Gavala M, Hill L, Bertics P (2009) Cell signaling via the P2X(7) nucleotide receptor: linkage to ROS production, gene transcription, and receptor trafficking. Purinergic Signal 5: 175–187.
7. Smart M, Gu B, Panchal R, Wiley J, Cromer B, et al. (2003) P2X7 receptor cell surface expression and cytolytic pore formation are regulated by a distal C-terminal region. J Biol Chem 278: 8853–8860.
8. Denlinger LC, Fisette PL, Sommer JA, Watters JJ, Prabhu U, et al. (2001) Cutting edge: the nucleotide receptor P2X7 contains multiple protein- and lipid-interaction motifs including a potential binding site for bacterial lipopolysaccharide. J Immunol 167: 1871–1876.
9. Wiley J, Dao-Ung L, Li C, Shemon A, Gu B, et al. (2003) An Ile-568 to Asn polymorphism prevents normal trafficking and function of the human P2X7 receptor. J Biol Chem 278: 17108–17113.
10. Denlinger L, Sommer J, Parker K, Gudipaty L, Fisette P, et al. (2003) Mutation of a dibasic amino acid motif within the C terminus of the P2X7 nucleotide receptor results in trafficking defects and impaired function. J Immunol 171: 1304–1311.
11. Bradley HJ, Liu X, Collins V, Owide J, Goli GR, et al. (2010) Identification of an intracellular microdomain of the P2X7 receptor that is crucial in basolateral membrane targeting in epithelial cells. FEBS Lett 584: 4740–4744.

12. Gavala ML, Hill LM, Lenertz LY, Karta MR, Bertics PJ (2010) Activation of the transcription factor FosB/activating protein-1 (AP-1) is a prominent downstream signal of the extracellular nucleotide receptor P2RX7 in monocytic and osteoblastic cells. J Biol Chem 285: 34288–34298.
13. Denlinger L, Coursin D, Schell K, Angelini G, Green D, et al. (2006) Human P2X7 pore function predicts allele linkage disequilibrium. Clin Chem 52: 995–1004.
14. Denlinger L, Angelini G, Schell K, Green D, Guadarrama A, et al. (2005) Detection of human P2X7 nucleotide receptor polymorphisms by a novel monocyte pore assay predictive of alterations in lipopolysaccharide-induced cytokine production. J Immunol 174: 4424–4431.
15. Lenertz L, Wang Z, Guadarrama A, Hill L, Gavala M, et al. (2010) Mutation of putative N-linked glycosylation sites on the human nucleotide receptor P2X(7) reveals a key residue important for receptor function. Biochemistry 49: 4611–4619.
16. Ulery PG, Rudenko G, Nestler EJ (2006) Regulation of DeltaFosB stability by phosphorylation. J Neurosci 26: 5131–5142.
17. Boumechache M, Masin M, Edwardson JM, Gorecki DC, Murrell-Lagnado R (2009) Analysis of assembly and trafficking of native P2X4 and P2X7 receptor complexes in rodent immune cells. J Biol Chem 284: 13446–13454.
18. Michelsen K, Yuan H, Schwappach B (2005) Hide and run. Arginine-based endoplasmic-reticulum-sorting motifs in the assembly of heteromultimeric membrane proteins. EMBO Rep 6: 717–722.
19. Staros JV (1982) N-hydroxysulfosuccinimide active esters: bis(N-hydroxysulfosuccinimide) esters of two dicarboxylic acids are hydrophilic, membrane-impermeant, protein cross-linkers. Biochemistry 21: 3950–3955.
20. Nicke A (2008) Homotrimeric complexes are the dominant assembly state of native P2X7 subunits. Biochem Biophys Res Commun 377: 803–808.
21. Feng YH, Li X, Wang L, Zhou L, Gorodeski GI (2006) A truncated P2X7 receptor variant (P2X7-j) endogenously expressed in cervical cancer cells antagonizes the full-length P2X7 receptor through hetero-oligomerization. J Biol Chem 281: 17228–17237.
22. Torres GE, Egan TM, Voigt MM (1999) Hetero-oligomeric assembly of P2X receptor subunits. Specificities exist with regard to possible partners. J Biol Chem 274: 6653–6659.
23. Larkin A, Imperiali B (2011) The expanding horizons of asparagine-linked glycosylation. Biochemistry 50: 4411–4426.
24. Van Craenenbroeck K (2012) GPCR Oligomerization: Contribution to Receptor Biogenesis. Subcell Biochem 63: 43–65.
25. Grunberg J, Sterchi EE (1995) Human lactase-phlorizin hydrolase: evidence of dimerization in the endoplasmic reticulum. Arch Biochem Biophys 323: 367–372.
26. Garcia-Huerta P, Diaz-Hernandez M, Delicado EG, Pimentel-Santillana M, Miras-Portugal MT, et al. (2012) The specificity protein factor Sp1 mediates transcriptional regulation of P2X7 receptors in the nervous system. J Biol Chem 287: 44628–44644.
27. Carle T, Ohnishi Y, Ohnishi Y, Alibhai I, Wilkinson M, et al. (2007) Proteasome-dependent and -independent mechanisms for FosB destabilization: identification of FosB degron domains and implications for DeltaFosB stability. Eur J Neurosci 25: 3009–3019.